Zirconium modified pomegranate peel for efficient removal of arsenite from water

Bhoj Raj Poudel[1,2], Dhan Shree Ale[2], Ram Lochan Aryal[1,3], Kedar Nath Ghimire[1], Surendra Kumar Gautam[2,] *, Hari Paudyal[1], Megh Raj Pokhrel[1]

[1]Central Department of Chemistry, Tribhuvan University, Kathmandu, Nepal
[2]Department of Chemistry, Tri-Chandra Multiple Campus, Tribhuvan University, Kathmandu, Nepal
[3]Department of Chemistry, Amrit Campus, Tribhuvan University, Kathmandu, Nepal

*Email: surendra.gautam@trc.tu.edu.np

ABSTRACT

We developed a novel biosorbent based on zirconium-modified pomegranate peel (SPP@Zr) for efficient arsenic (As(III)) removal from water. SEM, EDX, XRD, and FTIR were used to characterize the prepared biosorbent. The batch adsorption method was used to evaluate the adsorption viability of biosorbents for the removal of As(III) from water. The EDX analysis of saponified pomegranate peels (SPP) before and after Zr (IV) loading demonstrated that ion exchange was the preferred metal loading technique. As (III) adsorption is very pH-dependent, with the maximum adsorption occurring at pH 8.0. The maximum As(III) adsorption capacity of SPP@Zr was found to be 82.0 mg/g. According to isotherm and kinetic modeling studies, the experimental results fitted well with the Langmuir isotherm and pseudo-second-order kinetic modeling. The spent biosorbent may be easily regenerated and reused using an alkaline solution. Hence, SPP@Zr is proving to be a promising biosorbent for uptake of As (III) from water.

1. Introduction

Arsenic is a highly toxic naturally occurring element found in the earth's crust [1]. The natural occurrence of arsenic in groundwater is a serious concern worldwide due to its chronic toxicity and carcinogenicity [2, 3]. Arsenic contamination in groundwater has caused chronic health effects to millions of people throughout the world. [4]. In 1973, the Agency

for Toxic Substances and Disease Registry (ATSDR) has ranked arsenic as the number one toxic substance. The inorganic form of arsenic is classified as a Group 1 carcinogenic by the International Agency for Research on Cancer (IARC) [5, 6]. WHO and USEPA have recommended an allowable arsenic concentration of 10 ppb 0.01mg/L) in drinking water [7, 8]. Both organic and inorganic form of arsenic is found in the environment. The inorganic form of arsenic is more toxic than the organic form. The inorganic form of arsenic in an aqueous medium is arsenite (As(III)) or arsenate (As(V)) [9-11]. Arsenic is exposed to groundwater through natural and anthropogenic activities such as volcanic emission, geochemical activity, rock, and soil weathering, combustion of fossil fuels, mining activities, agricultural chemicals, wood preservatives, industrial discharges, electroplating, pigments, dyestuffs, and paints [12-14]. Several treatment techniques, such as coagulation-filtration [15], ion exchange [16], reverse osmosis [17], and adsorption [18, 19] are reported for As(III) removal from aqueous medium. Compared to others, adsorption looks more promising for the removal of trace concentration of contaminants due to cost-effectiveness, easy and simple operation, minimum production of secondary products [10, 20].

Several agro waste-based products have been utilized by numerous researchers in the past to remove arsenic [1, 21-24]. Zirconium (Zr) is a multivalent transition metal that has recently been widely investigated for wastewater treatment processes. This increased focus might be owing to the capacity of zirconium to be impregnated onto biosorbents via interactions with functional groups. Zirconium impregnation into biosorbents has been demonstrated to be effective in the high-selectivity removal of PO_4^{3-}, F^-, and As(III)/As(V) [25-27]. Furthermore, because Zr is prevalent in the earth's crust, it might be readily accessible for environmental media rehabilitation. As a result, Zr was chosen for

removal of As(III) using our previously proposed adsorbent, pomegranate peels [9]. Using common agro-waste, pomegranate peels, we examined a novel form of the adsorbent substitute to conventional synthetic ion exchangers for As(III) ion remediation. It's frequently dumped as a waste residue and may be found for free or very cheap. Due to the presence of cellulose/hemicellulose, pectin, and lignin as significant ingredients and adequate hydroxyl, carboxyl, and carbonyl functional groups, it might be employed as an efficient biosorbent. This biopolymer contains 10-15% pectin, making it an excellent source of natural pectin [28]. To the best of our knowledge, this is the first study to look at the potential of Zr(IV) impregnated saponified pomegranate peel (SPP@Zr) for adsorption of trace concentrations of As(III) from water.

The objective of this study was to investigate into the biosorption properties of the prepared novel SPP@Zr toward As(III) ions in water. Its adsorption kinetics and isotherms were investigated. The batch method was used to investigate the effect of various factors such as initial pH, adsorption time, and coexisting ions on the uptake of As(II) by the SPP@Zr. Combining experimental data and characterization results yielded the mechanisms of As(III) biosorption onto SPP@Zr.

2. Materials and Methods
2.1. Materials

The pomegranate peel was washed in distilled water several times, chopped into pieces, and dried. The dried peel pieces were then crushed with a crusher, sieved to enable pass through a 120 μ mesh, and then desiccated in a hot air oven at 60-70°C for 24 hours. The dry powder prepared in this way was termed raw pomegranate peels hereafter abbreviated as RPP. Chemicals of analytical grade were utilized without further purification.

All the solutions were made with deionized (DI) water. The zirconium oxychloride octahydrate,

calcium hydroxide, and sodium arsenite were acquired from Sigma-Aldrich, New Delhi, India.

2.2. Preparation of the Zr (IV)-loaded saponified pomegranate peel

The adsorbent (SPP@Zr) was synthesized by the method given by our previous work. The synthesis procedure has been described in detail elsewhere [9].

2.3. Characterization

The morphology and elemental composition of adsorbent were studied by scanning electron microscopy (SEM; JEOL, JSM-6701F, Japan) with an energy dispersive X-ray (EDX). X-ray diffraction (XRD) patterns were utilized to evaluate the crystallinity of the biosorbent using an X-ray diffractometer (Rigaku Co., Japan). Fourier transform infrared (FTIR) spectroscopy (IR Affinity -1S-SHIMADZU spectrometer, Kyoto, Japan) was used to examine the surface functional groups of the as-prepared biosorbent.

2.4. Adsorption experiments

Batch experiments were used to assess the effects of the pH of the solution, adsorption kinetics, adsorption isotherm, and the influence of competitive ions. Desorption tests were carried out to determine the adsorbent's reusability and regeneration capability.

For the kinetics study, 25 mg SPP@Zr were added into flasks having 25 mL of 28.32 mg/L arsenite solution. The pH was maintained at 8.0 utilizing 0.1 M HNO_3 and 0.1 M NaOH. The contents were stirred at 120 rpm using a shaker at room temperature. The equilibrium adsorption capacity (q_e), adsorption capacity (q_t) at a predetermined time (t), and % adsorption (%A) of As(III) ions were evaluated according to Eqs. (1), (2), and (3), respectively.

$$q_e = \frac{(C_o - C_e)\,V}{m} \qquad (1)$$

$$q_t = \frac{(C_o - C_t)\,V}{m} \qquad (2)$$

$$\%A = \frac{(C_o - C_e)}{C_o} \times 100 \qquad (3)$$

where q_e and q_t represent the adsorption capacity (mg g^{-1}) at equilibrium and at a preselected time, respectively; C_0, C_e, and C_t represent the concentrations of arsenic (mg/L) in initial, at equilibrium, and at a predetermined time (t), respectively, V denotes the volume of solution (mL), and m is the mass of SPP@Zr used (g). The pseudo-first-order [29] and pseudo-second-order [30] kinetic models were fitted using Eq. (4) and Eq. (5), respectively, to the experimental results to further elucidate the adsorption mechanism.

$$log\,(q_e - q_t) = log\,q_e - \frac{k_1}{2.303}\,t \qquad (4)$$

$$\frac{t}{q_t} = \frac{1}{k_2 q_e^2} + \frac{1}{q_e}\,t \qquad (5)$$

where q_e represents the equilibrium sorption efficiency, k_1 (min^{-1}) and k_2 (g/mg . min) are the rate constants of pseudo-1st-order and pseudo-2nd-order, correspondingly.

In adsorption isotherms studies, 25 mg SPP@Zr was taken in various conical flasks having 25 mL As(III) solutions (10 to 500 mg/L). The flasks were stirred for 8 hours at room temperature. Then, samples were filtered and examined for initial and final concentrations of arsenite. The As(III) adsorption performances were described by two isotherm models, Langmuir [31] and Freundlich [32] using Eq. (6) and Eq. (7), respectively.

$$\frac{C_e}{q_e} = \frac{1}{q_m\,b} + \frac{C_e}{q_m} \qquad (6)$$

$$log\,q_e = log\,K_F + \left(\frac{1}{n}\right) log\,C_e \qquad (7)$$

where q_m (mg/g) is the maximum adsorption capacity, b (L/mg) is the Langmuir equilibrium constant, K_F [(mg/g)(L/mg)$^{1/n}$] is the Freundlich constant for sorption capacity, and 1/n is the dimensionless heterogeneity factor for adsorption intensity. In addition, a

dimensionless separation factor (R_L) was used to investigate the important aspects of the Langmuir model [33], which may be represented by Eq. (8):

$$R_L = \frac{1}{1 + (bC_o)} \qquad (8)$$

The R_L value infers the phenomenon of the Langmuir isotherm. If R_L is $0 < R_L < 1$ (favorable), while $R_L > 1$ (unfavorable), $R_L = 1$ (linear), and $R_L = 0$ (irreversible) adsorption process [34].

The effect of solution pH on As(III) adsorption was evaluated over the wide pH range. 25 mL solution of 25 mg/L As(III) stock solution was taken in the conical flask. After pH adjustment to a predetermined value (2-13), 25 mg of SPP@Zr was added to each flask. The solutions were shaken for 8 hrs. at room temperature. The equilibrium concentration of As(III) after adsorption was measured. Three levels of concentrations of each competitive ion were added to 25 mg/L As(III) solution to study the impact of common coexisting anions (Cl$^-$,

SO$_4{}^{2-}$, and PO$_4{}^{3-}$) on the removal of As(III). Furthermore, the blank sample was made using the same procedure but without the addition of coexisting anion. 0.1 M HNO$_3$ and 0.1 M NaOH were used to keep the pH of the whole solution at 8. The biosorbent dose of 1 g/L was added and agitated for 8 hours at room temperature. For As(V) analysis, the filtrates were collected.

The reusability of the as-prepared adsorbents was tested using four cycles of adsorption-desorption of As(III). After washing the spent biosorbents with 0.1 M NaOH solution, the reusability of the adsorbents was tested. To test reusability, the regenerated adsorbent was used for up to four cycles.

2.5. Analysis

The concentrations of As (III) in the samples were evaluated using an inductively coupled plasma mass spectrometer (ICP-MS, Agilent 7900, Santa Clara, CA, USA), while the pH of the solution was measured using a pH meter (CHEMI LINE CL-180, Indiamart, India).

3. RESULTS AND DISCUSSION

3.1. Characterization of the adsorbents

Fig. 1 represents the SEM images and EDS spectra of SPP, SPP@Zr, and As(III) adsorbed SPP@Zr. In the SEM images of The surfaces of SPP (Fig. 1(a)) and Zr (IV)-SPP (Fig. 1(b)), the surfaces showed rough and uneven with micro and mesopores, which possibly provide binding sites for adsorption of As (III) physically as well as chemically and favored the adsorption of As (III). SEM image of As (III)-SPP@Zr (Fig. 1(c)) shows that the pores are partially covered by the adsorbed As (III) ion, which creates a layer that settles on the rough surfaces. In the EDX of SPP (Fig. 1(d)), the intense peaks of Ca indicate that Ca is one of the major elements of the saponification product. After Zr (IV) loading (Fig. 1(e)) peaks of Ca were decreased and the new peak corresponding to Zr was appeared, which is strong evidence of the exchange of Ca^{2+} ions from SPP with Zr (IV) ion during loading reaction through cation exchange mechanism. In the case of As (III) adsorbed Zr (IV)-SPP biomass (Fig. 1(f)), a new additional peak of arsenic has appeared. From this, it was evaluated that highly accommodation of As (III) ion onto the surface with ligand exchanged between hydroxyl ion and arsenic anion as depicted in Scheme 2. The elemental composition of SPP, SPP@Zr, and As(III) adsorbed SPP@Zr are shown in Table 1.
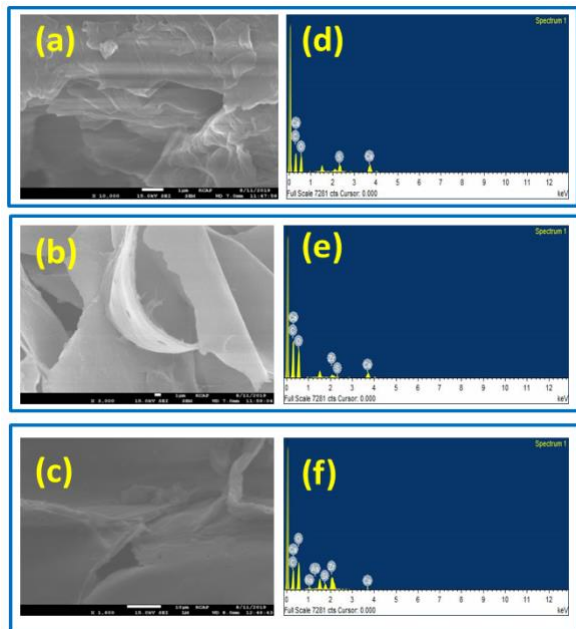
Fig.1. SEM images of (a) SPP, (b) SPP@Zr, (c) As (II)-SPP@Zr, and EDS spectra of (d) SPP, (e) SPP@Zr, (f) As (III)- SPP@Zr.

Table 1. Elemental composition of SPP, SPP@Zr, and As(III) adsorbed SPP@Zr.

Elements	SPP (Wt %)	SPP@Zr (Wt%)	As-SPP@Zr (Wt %)
C K	41.29	44.72	38.62
O K	43.82	40.36	41.01
Na K	ND	ND	0.42
Si K	ND	ND	2.12
Ca K	13.89	0.56	0.46
As L	ND	ND	3.87
Zr L	ND	14.35	13.49
Total	100.00	100.00	100.00

The XRD curve of SPP@Zr is shown in Fig. 2(a), where sharp peaks corresponding to the crystalline structure are not observed indicating the amorphous nature of the prepared adsorbent. In the FTIR spectra of RPP (Fig. 2(b)), a broad and strong peak located at around 3345 cm^{-1} is due to –OH stretching vibration [9]. The small peak at 2923 cm^{-1} is associated with the vibrations of –CH and –CH$_2$ units. [35]. The peaks at roughly 1729 and 1613 cm^{-1} relate to the –COO and C=O groups, correspondingly. The C=O stretching of the carboxylic groups is responsible for the peak at 1629 cm^{-1}. The prominent peak seen at roughly 1015 cm^{-1} corresponds to –C–O– linkages. After saponification (in SPP), the peak observed at around 1729 cm-1 is disappeared, and a new peak appeared at around 1607 cm-1, indicating the formation of calcium carboxylate. The peak moved to 1626 cm-1 after impregnation with Zr(IV) (in SPP@Zr), which is owing to the replacement of greater molecular weight Zr(IV) for lower molecular weight Ca (II). Furthermore, the intense peak at around 1076 cm^{-1} is associated with –Zr-OH bonds [36]. It shows that Zr(IV) was successfully loaded onto the biomass surface. Afterward, As(III) biosorption, the peak at around 1076 cm^{-1} (Zr–OH) was decreased, and a new band was found at 815 cm^{-1} for Zr–O–As vibration, showing that the hydroxyl groups were exchanged by the oxyanions of As(III).
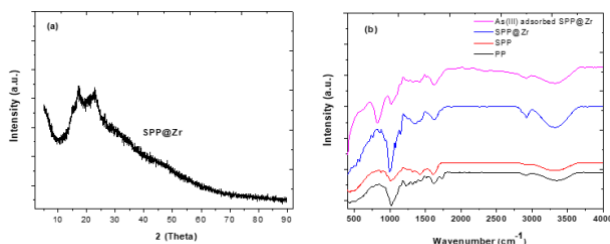

Fig. 2. (a) XRD pattern of SPP@Zr; (b) FT-IR of PP, SPP, SPP@Zr before and after As(III) biosorption.

3.2. Biosorption experiments

3.2.1. Effect of the pH of the solutions

As(III) adsorption onto RPP and SPP@Zr has been investigated in the pH range of 2.0 – 13.0. According to the findings, the % adsorption of As(III) increases progressively from pH 2.0 to pH 8.0, then drops to pH 13. The adsorption of As(III) was the most favorable at pH 7.0 to 10.0

for SPP@Zr as shown in Fig 3. The removal efficiency of As(III) was highest at pH 8.0. As a result, pH 8.0 was selected as the optimal pH for further adsorption test of As(III). Depending on the chemistry of the aqueous solution, As(III) occurs primarily as a neutral species (H_3AsO_3) at pH 7.0, while as an anionic species ($H_2AsO_3^-$, and $HAsO_3^{2-}$) at pH 7.0- 12.0, and as AsO_3^{3-} species at pH >12.0 [18]. The ligand exchange interaction between hydroxyl ions of SPP@Zr and neutral As(III) species, i.e. H_3AsO_3, is not favourable at lower pH, resulting in minimal biosorption. At pH approximately 8.0, the anionic species of As(III) predominate, making the exchange of hydroxyl ions by the oxyanion of As(III) more favourable, resulting in increased adsorption of As(III). Due to competition between oxyanions of As(III) and hydroxide ions at higher pH, As(III) biosorption might be inhibited. When compared to SPP@Zr, the adsorption of As(III) using RPP was found to be significantly poor even at optimum pH. As a result, for the subsequent experiments, only SPP@Zr was chosen as the adsorbent.
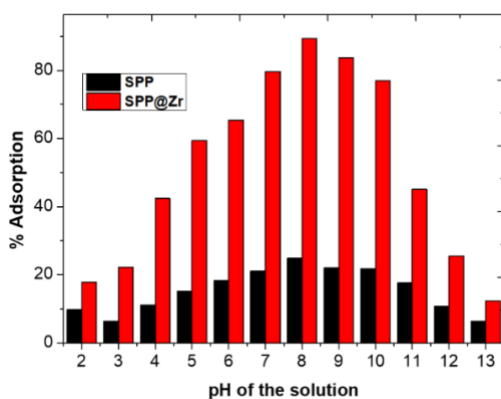
studied at optimum pH of 8.0 and the results are revealed in Fig. 4 (a). The adsorption of As(III) increases rapidly at the beginning up to 1 h, whereas it becomes steady and finally attained equilibrium after 3 h. Because the equilibrium was attained in less than 3 hours, the contact period in further tests was set at 8 hours to assure full sorption. The pseudo-first-order and pseudo-second-order models were fitted to the kinetic data to better clarify the kinetic process. According to Eqs. (4) and (5), two plots Fig. 4(b) and Fig. 4(c) were drawn. Table 2 shows the estimated values of kinetic parameters as well as the regression coefficient (R^2). The pseudo-2nd-order model had an R^2 of 0.999, which was nearer to unity than the pseudo-1st-order model. Furthermore, in the pseudo-second-order kinetic, the calculated equilibrium adsorption capacity (q_e (cal) = 25.25 mg/g) is close to the experimental value (q_e (exp)) = 24.98 mg/g. As a result, the As(III) biosorption on SPP@Zr followed pseudo-second-order kinetics, signifying that chemisorption may be dominating the biosorption of As(III).
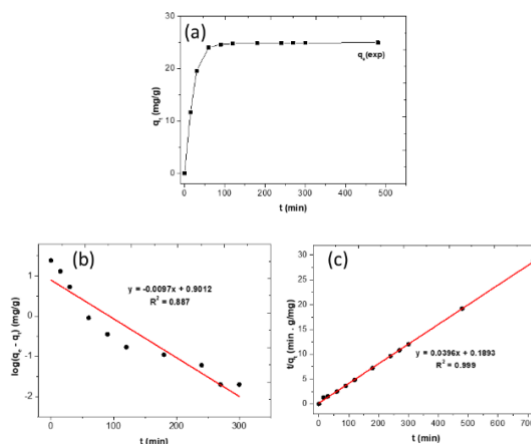

Fig. 4. Adsorption kinetics study of As(III): (a) q_t versus contact time; (b) pseudo-first-order kinetics plot of SPP@Zr with As(III) system; (c) pseudo-second-order kinetics plot of SPP@Zr with As(III) system.

Fig. 3. Effect of solution pH on As(III) biosorption onto SPP and SPP@Zr.

3.2.2. Adsorption kinetics

The influence of interaction time for the removal of aqueous As(III) by SPP@Zr was

Table 2. Kinetics parameters for As(III) biosorption onto SPP@Zr.

Order	R^2	q_e (exp) (mg/g)	q_e (cal) (mg/g)	k_1 (min^{-1})	k_2 (g/mg . min)
Pseudo-second- order	0.999	24.98	25.25	-	8.30×10^{-3}
Pseudo-first-order	0.887	24.98	7.96	22.3×10^{-3}	-

3.2.3. Adsorption isotherms

The adsorption isotherm was described by evaluating the fluctuation of starting As(III) concentration for adsorption capacity. Figure 5(a) shows the adsorption isotherms of As(III) onto SPP@Zr at pH 8.0 and room temperature. The results show that when the As(III) ion concentration raised from low to high, the adsorption capacity increased fast, with a slow but steady rise until saturation (plateau) was reached at high concentrations. The increased adsorption rate early on might be explained by the increasing availability of vacant sorption sites in the adsorbent. At a high concentration area, the adsorption capacity achieved a plateau, indicating that no more sites are available for sorption. The adsorption data were studied utilizing Langmuir (Eq. 6) and Freundlich (Eq. 7) models to explain the As(III) biosorption performance. Isotherm's parameters were determined from the slope and intercept of the respective plots, C_e/q_e vs C_e (Fig. 5(b)) and $\log q_e$ vs $\log C_e$ (Fig. 5(c)), respectively. The estimated isotherm parameters with R^2 value are listed in Table 3.

Table 3. Isotherms parameters for As(III) biosorption onto SPP@Zr.

|	Parameter	Value
Langmuir isotherm	q_m (mg g^{-1})	72.52
	b (L mg^{-1})	0.064
	R^2	0.998
Freundlich isotherm	K_F (mg g^{-1}) (L mg^{-1})$^{1/n}$	12.12
	$1/n$	0.323
	R^2	0.937

The greater R^2 indicated that the Langmuir model was more suited to describe the biosorption behaviour of As(III) onto SPP@Zr, as shown in Table 2. We concluded that biosorption processes took occur on the adsorbent's surface, which was referred to as monolayer adsorption. The calculated maximum adsorption capacity (q_m) of SPP@Zr for As(III) was 72.52 mg/g, which provided a substantial potential for practical aqueous removal of As(III) in comparison with several other biosorbents reported in past research in discussion (Table 4).

Table 4. Comparison of As(III) biosorption capacities of various biosorbents with SPP@Zr.

Adsorbent	Optimal pH	q_m (mg/g)	Reference
Zr(IV)-loaded apple peels	9.0	15.68	[37]
La(III)-loaded saponified watermelon rind	12.08	37.73	[38]
Zr-chitosan modified sodium alginate composite	-	43.19	[39]
Powdered almond shell	7.2	4.6	[40]
Modified hazelnut shell	9.0	11.84	[41]
Iron-coated seaweeds	7.0	4.2	[42]
ZrO$_2$-coated sawdust	7.0	29.0	[43]
La$_2$O$_3$-coated sawdust	7.0	22.0	[43]
Iron dopped amino-functionalized sawdust	7.0	10.1	[44]
SPP@Zr	8.0	72.52	This study

Furthermore, the values of R_L derived from Eq. (8) are shown in Fig. 5(d). The derived R_L values ranged from 0 to 1, indicating that As(III)

biosorption onto SPP@Zr is favourable and that the adsorbate-adsorbent surface bonding is
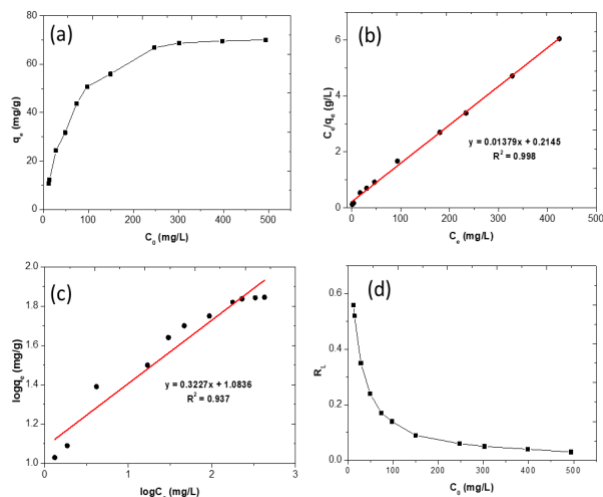
strong.

Fig. 5. (a) Equilibrium adsorption capacity for As(III) onto SPP@Zr at various initial concentrations of As(III); (b) Linearized Langmuir isotherm plot of SPP@Zr with As(III) system; (c) Linearized Freundlich isotherm plot of SPP@Zr with As(III) system; (d) Value of R_L as a function of initial concentration of As(III).

3.2.4. Influence of coexisting ions

The influence of various coexisting ions for the removal of As(III) ions was investigated, and the findings are shown in Fig. 6. In the presence of Cl^-, and SO_4^{2-} at any concentration level, a small drop in % adsorption of As(III) occurs, as seen in the figure compared to the blank. This might be because these ions have a lower binding capability than As(III) ions. The inclusion of PO_4^{3-}, on the other hand, drastically reduced As(V) adsorption, owing to severe competition between phosphate and arsenite ions for the adsorbent's binding sites. At a phosphate concentration level of 75 mg L^{-1}, the adsorption of arsenate drops by ~ 40%. Furthermore, the chemical and structural resemblances of arsenite with phosphate in an aquatic environment account for the dramatic decrease in As(III) adsorption in the presence of phosphate.
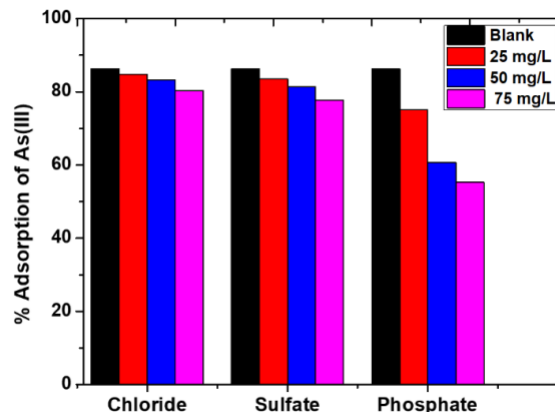

Fig. 6. Effect of coexisting anions for the adsorption of As(III) ions on SPP@Zr.

3.2.5. Desorption and reusability of adsorbent

The As(III) ion is weakly sorbed onto the biosorbent at pH > 11, so elution of As(III) from spent biosorbent may be accomplished with ease utilizing NaOH solution. As a result, the spent SPP@Zr can be revived for recycling using a 0.1 M NaOH solution. The adsorbed arsenite anion may have been swapped via ligand exchange reaction by hydroxyl ions in the alkali solution. For reusability, the SPP@Zr regenerated by NaOH was washed with distilled water until neutrality. A reusability investigation of the biosorbent was performed after desorption for up to four cycles. After four consecutive cycles, the As(III) adsorption capacity of SPP@Zr decreased from 86.4% to 67.3% percent, as shown in Fig. 7. Even after the fourth consecutive cycle, the As(III) removal efficiency was more than 67%, showing that SPP@Zr was highly recyclable and a viable adsorbent for removing As(III) from an aqueous solution.
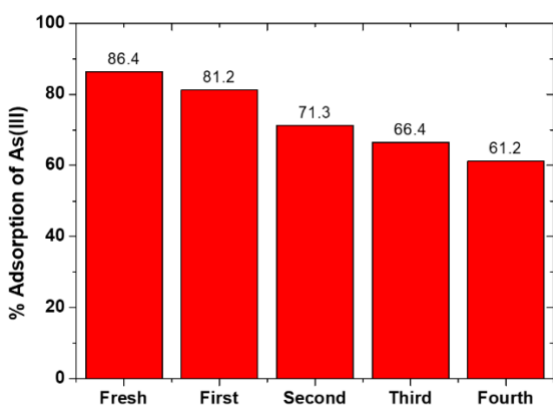
Fig. 7. The % adsorption of As(III) onto SPP@Zr in the subsequent adsorption-desorption cycle.

3.2.6. As(III) biosorption/desorption mechanism

The As(III) biosorption on SPP@Zr closely matched the pseudo-second-order kinetic, implying that the process is chemisorption-driven. The FTIR spectra of biosorbent before and after As(III) adsorption supported this hypothesis. The band at 1076 cm^{-1} (Zr–OH) was decreased after sorption, and a new band for Zr–O–As a vibration was found at about 815 cm^{-1}, showing that the –OH group was substituted by oxyanion of As(III). The ligand exchange process for As(III) biosorption utilizing SPP@Zr is as follows. In the removal of anionic pollutants, the loaded Zr(IV) metal ion plays a crucial role. After zirconium is loaded onto SPP, it forms stable chelates with pectic acid (Biswas et al. 2008). Due to the steric hindrance of a large polymer of pectic acid, all the positive charges of the zirconium ions are not entirely counterbalanced by the negatively charged carboxylic group. The carboxylic group neutralizes just one or two positive charges of Zr(IV), with the remaining neutralized by negatively charged hydroxide ions, which are plentiful in the water. A ligand exchange process was anticipated to exchange these hydroxide ions with oxyanions of As(III). Adsorbed As(III) may also be readily eluted

utilizing NaOH solution via a ligand exchange reaction between the adsorbed oxyanions of As(III) and hydroxide ions in the solution. The mechanism of the ligand exchange process through As(III) adsorption-desorption is depicted in Scheme 1.
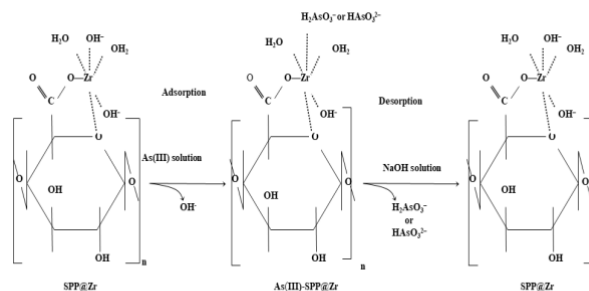
Scheme 1. Adsorption and desorption mechanism for As(III) onto SPP@Zr.

CONCLUSIONS

SPP@Zr was synthesized and used as an effective biosorbent for removing arsenic from water in this study. Based on the results of the characterizations, it was acceptable to conclude that efficient loading of Zr (IV) into biomass and efficacious biosorption of As (III) onto SPP@Zr were achieved. The maximum adsorption of As(III) on SPP@Zr was evaluated at pH 8.0. The biosorption trailed a pseudo-second-order kinetic, implying that the process was chemisorption with higher initial adsorption rates. The Langmuir model fit the equilibrium data better, indicating that monolayer adsorption occurred on a homogeneous surface of the SPP@Zr. The maximum adsorption capacity was evaluated as 72.52 mg/g, which was found to be higher than several other biosorbents found in the literature. Furthermore, SPP@Zr works well in the presence of a variety of coexisting anions, and the spent adsorbent is easily regenerated and reused for up to four consecutive cycles. As a result, SPP@Zr can be considered a useful, cost-

effective, environmentally friendly, and reusable biosorbent for removing As(III) from aqueous solutions.

Acknowledgments

References

[1] S. Irem, E. Islam, Q. Mahmood Khan, M. Anwar ul Haq, A. Jam al Hashmat, Adsorption of arsenic from drinking water using natural orange waste: kinetics and fluidized bed column studies, Water Sci. Technol. Water Supply 17 (2017) 1149-1159. https://doi.org/10.2166/ws.2017.009

[2] B.R. Poudel, R.L. Aryal, S. Bhattarai, A.R. Koirala, S.K. Gautam, K.N. Ghimire, B. Pant, M. Park, H. Paudyal, M.R. Pokhrel, Agro-waste derived biomass impregnated with TiO_2 as a potential adsorbent for removal of As (III) from water, Catalysts 10(2020)1125. https://doi.org/10.3390/catal10101125

[3] J. Podgorski, M. Berg, Global threat of arsenic in groundwater, Science 368 (2020)845–850. https://doi.org/10.1126/science.aba1510

[4] C. Prum, R. Dolphen, P. Thiravetyan, Enhancing arsenic removal from arsenic-contaminated water by Echinodorus cordifolius-endophytic Arthrobacter creatinolyticus interactions, J. Environ. Manage.213(2018)11-19. https://doi.org/10.1016/j.jenvman.2018.02.060

[5] D.N. Nhiem, D.H. Duc, D.T. Lim, N.Q. Bac, P.N. Chuc, D.T. Dung, N.T.H. Chi, N.N. Pham, N.V.N. Mai, T.X. Mau, D.Q. Khieu, Strong adsorption of arsenite and phosphate from aqueous solution using La_2O_3–CeO_2 composite, J. Polym. Environ. 29(2021)1310–1323. https://doi.org/10.1007/s10924-020-01967-6

[6] T.T.Q. Nguyen, P. Loganathan, T.V. Nguyen, S. Vigneswaran, H.H. Ngo, Iron and zirconium modified luffa fibre as an effective bioadsorbent to remove arsenic from drinking water, Chemosphere 258 (2020)127370. https://doi.org/10.1016/j.chemosphere.2020.127370

[7] World Health Organization (WHO). 2011. Arsenic in Drinking-water Background Document for Development of WHO Guidelines for Drinking-water Quality. http://www.who.int/water_sanitation_health/dwq/chemicals/arsenic.pdf

[8] United States Environmental Protection Agency (USEPA). 2017. Drinking Water Requirements for States and Public Water System. https://www.epa.gov/dwreginfo/chemical--contaminant--rules

[9] B.R. Poudel, R.L. Aryal, S.K. Gautam, K.N. Ghimire, H. Paudyal, M.R. Pokhrel, Effective remediation of arsenate from contaminated water by zirconium modified pomegranate peel as an anion exchanger, J. Environ. Chem. Eng. 9 (2021)106552. https://doi.org/10.1016/j.jece.2021.106552

[10] D. Mohan, C.U. Pittman Jr, Arsenic removal from water/wastewater using adsorbents-a critical review, J. Hazard. Mater.142(2007)1–53, https://doi.org/10.1016/j.jhazmat.2007.01.006

[11] M.R. Hadiani, K. Khosravi-Darani, N. Rahimifard, Optimization of As (III) and As (V) removal by Saccharomyces cerevisiae biomass for biosorption of critical levels in the food and water resources, J. Environ. Chem. Eng. 7 (2019)102949. https://doi.org/10.1016/j.jece.2019.102949

[12] K. Shehzad, M. Ahmad, J. He, T. Liu, W. Xu, J. Liu, Synthesis of ultra-large ZrO2 nanosheets as novel adsorbents for fast and efficient removal of As (III) from aqueous solutions, J. Colloid Interface Sci. 533(2019)588-597. https://doi.org/10.1016/j.jcis.2018.08.079

[13] S. Karki, R.L. Aryal, S. Bhattarai, S.K. Gautam, B.R. Poudel, Adsorptive Removal of arsenic (III) from aqueous solution using chemically-modified sweet lime (Citrus limetta) peels, J. Nep. Chem. Soc.37(2017)11-19. https://doi.org/10.3126/jncs.v37i0.32044

[14] M. Imran, M.M. Iqbal, J. Iqbal, N.S. Shah, Z.U.H. Khan, B. Murtaza, M. Amjad, S. Ali, M. Rizwan, Synthesis, characterization, and application of novel MnO and CuO impregnated biochar composites to sequester arsenic (As) from water: modeling, thermodynamics, and reusability, J. Hazard. Mater. 401 (2021) 123338. https://doi.org/10.1016/j.jhazmat.2020.123338

[15] S.R. Wickramasinghe, B. Han, J. Zimbron, Z. Shen, M.N. Karim, Arsenic removal by coagulation and filtration: comparison of groundwaters from the United States and Bangladesh, Desalination,169(2004)231–244. https://doi.org/10.1016/j.desal.2004.03.013

[16] A. Ortega, I. Oliva, K.E. Contreras, I. González, M.R. Cruz-Díaz, E.P. Rivero, Arsenic removal from water by hybrid electro-regenerated anion exchange resin/electrodialysis process, Sep. Purif. Technol.184(2017)319–326. https://doi.org/10.1016/j.seppur.2017.04.050

[17] A. Abej´on, A. Garea, A. Irabien, Arsenic removal from drinking water by reverse osmosis: Minimization of costs and energy consumption, Sep. Purif. Technol. 144 (2015)46–53. https://doi.org/10.1016/j.seppur.2015.02.017

[18] L. Hao, M. Liu, N. Wang, G. Li, A critical review on arsenic removal from water using iron-based adsorbents, RSC Adv. 8 (2018)39545–39560. https://doi.org/10.1039/C8RA08512A

[19] R.M. Dhoble, S. Lunge, A.G. Bhole, S. Rayalu, Magnetic binary oxide particles (MBOP): a promising adsorbent for removal of As (III) in water, Water Res. 45 (16)(2011)4769–4781. https://doi.org/10.1016/j.watres.2011.06.016

[20] A. Shrestha, B.R. Poudel, M. Silwal, M.R. Pokhrel, Adsorptive removal of phosphate onto iron loaded litchi chinensis seed waste, J. Inst. Sci.Technol. 23 (2018), 81-87. https://doi.org/10.3126/jist.v23i1.22200

[21] H. Tajernia, T. Ebadi, B. Nasernejad, M. Ghafori, Arsenic removal from water by sugarcane bagasse: an application of response surface methodology (RSM). Water Air Soil Pollut. 225 (2014) 1-22. https://doi.org/10.1007/s11270-014-2028-4

[22] K.R. Raj, A. Kardam, S. Srivastava, Development of polyethylenimine modified Zea mays as a high capacity biosorbent for the removal of As (III) and As (V) from aqueous system, Int. J. Miner. Process.122(2013)66-70. https://doi.org/10.1016/j.minpro.2013.02.010

[23] K.N. Ghimire, K. Inoue, H. Yamaguchi, K. Makino, T. Miyajima, Adsorptive separation of arsenate and arsenite anions from aqueous medium by using orange waste. Water Res. 37 (2003) 4945–4953. https://doi.org/10.1016/j.watres.2003.08.029

[24] V.M. Boddu, K. Abburi, J.L. Talbott, E.D. Smith, R. Haasch, Removal of arsenic (III) and arsenic (V) from aqueous medium using chitosan-coated biosorbent, Water Res.42(2008)633-642. https://doi.org/10.1016/j.watres.2007.08.014

[25] H. Paudyal, B. Pangeni, K. Inoue, H. Kawakita, K. Ohto, K.N. Ghimire, H. Harada, S. Alam, Adsorptive removal of trace concentration of fluoride ion from water by using dried orange juice residue, Chem. Eng. J. 223 (2013) 844–853. https://doi.org/10.1016/j.cej.2013.03.055

[26] B.K. Biswas, J.I. Inoue, K. Inoue, K.N. Ghimire, H. Harada, K. Ohto, H. Kawakita, Adsorptive removal of As (V) and As (III) from water by a Zr (IV)-loaded orange waste gel, J. Hazard. Mater. 154(2008)1066–1074. https://doi.org/10.1016/j.jhazmat.2007.11.030

[27] R.L. Aryal, K.P. Bhurtel, B.R. Poudel, M.R. Pokhrel, H. Paudyal, K.N. Ghimire, Sequestration of phosphate from water onto modified watermelon waste loaded with Zr (IV), Sep. Sci. Technol. (2021) 1–13. https://doi.org/10.1080/01496395.2021.1884878

[28] Z. Yang, T. Nisar, Y. Hou, Pomegranate peel pectin can be used as an effective emulsifier, Food Hydrocoll. 18 (2018) 30–35. https://doi.org/10.1016/j.foodhyd.2018.06.042

[29] S. Lagergren, Zur theorie der sogenannten adsorption geloster stoffe. 24(1898) 1-39.

[30] Y.S. Ho, Review of second-order models for adsorption systems, J. Hazard. Mater. 136(2006)681-689. https://doi.org/10.1016/j.jhazmat.2005.12.043

[31] I. Langmuir, The constitution and fundamental properties of solids and liquids, J. Am. Chem. Soc. 38 (1916) 2221–2295. https://doi.org/10.1021/ja02268a002

[32] H.M.F. Freundlich, Uber die adsorption in losungen, J. Phys. Chem. 57 (1906) 385–470. https://doi.org/10.1515/zpch–1907–5723

[33] J. Wang, X. Guo, Adsorption isotherm models: Classification, physical meaning, application and solving method, Chemosphere(2020)127279. https://doi.org/10.1016/j.chemosphere.2020.127279

[34] M.A. Al-Ghouti, D.A. Da'ana, Guidelines for the use and interpretation of adsorption isotherm models: A review. J. Hazard. Mater. 393(2020)122383. https://doi.org/10.1016/j.jhazmat.2020.122383

[35] A.Gupta,S.R.Vidyarthi,N.Sankararamakrishnan,Concurrent removal of As (III) and As (V) using green low-cost functionalized biosorbent-Saccharum officinarum bagasse. J. Environ. Chem. Eng.3(2015)113–121. https://doi.org/10.1016/j.jece.2014.11.023

[36] M.A. Rahman, D. Lamb, M.M. Rahman, M. M. Bahar, P. Sanderson, S. Abbasi, A.F. Bari, R. Naidu, Removal of arsenate from contaminated waters by novel zirconium and zirconium-iron modified biochar, J. Hazard. Mater. 409 (2021) 124488. https://doi.org/10.1016/j.jhazmat.2020.124488

[37] R. Mallampati, S. Valiyaveettil, Apple Peels-A Versatile Biomass for Water Purification? ACS Appl. Mater. Interfaces 5(2013),4443-4449. https://doi.org/10.1021/am400901e

[38] R.L. Aryal, A. Thapa, B.R. Poudel, M.R. Pokhrel, B. Dahal, H. Paudyal, K.N. Ghimire, Effective biosorption of arsenic from water using La (III) loaded carboxyl functionalized watermelon rind, Arab. J. Chem.15(2022)103674. https://doi.org/10.1016/j.arabjc.2021.103674

[39] S. Lou, B. Liu, Y. Qin, Y. Zeng, W. Zhang, L. Zhang, Enhanced removal of As (III) and As (V) from water by a novel zirconium-chitosan modified spherical sodium alginate composite, Int. J. Biol. Macromol. 176(2021)304–314.

https://doi.org/10.1016/j.ijbiomac.2021.02.077

[40] S. Ali, M. Rizwan, M.B. Shakoor, A. Jilani, R. Anjum, High sorption efficiency for As (III) and As (V) from aqueous solutions using novel almond shell biochar, Chemosphere 243(2020) 125330. https://doi.org/10.1016/j.chemosphere.2019.125330

[41] S. Sert, A. Celik, V.N. Tirtom, Removal of arsenic (III) ions from aqueous solutions by modified hazelnut shell, Desalin. Water Treat.75(2017)115-123. https://doi.org/10.5004/dwt.2017.20725

[42] B.R. Vieira, A.M. Pintor, R.A. Boaventura, C.M. Botelho, S.C. Santos, Arsenic removal from water using iron-coated seaweeds, J. Environ. Manag. 192(2017)224-233. https://doi.org/10.1016/j.jenvman.2017.01.054

[43] Setyono, D.; Valiyaveettil, S., Chemically modified sawdust as renewable adsorbent for arsenic removal from water. ACS Sustain. Chem. Eng. 2 (2014) 2722-2729. https://doi.org/10.1021/sc500458x

[44] L. Hao, T. Zheng, J. Jiang, G. Zhang, P. Wang, Removal of As (III) and As (V) from water using iron doped amino functionalized sawdust: characterization, adsorptive performance and UF membrane separation, Chem. Eng. J. 292(2016)163-173. https://doi.org/10.1016/j.cej.2016.01.097